DETC2013-12898

TRAVERSABILITY ANALYSIS OF A NOVEL ONE-DOF ROBOTIC LEG

Lionel Birglen
Robotics Laboratory
Department of Mechanical Engineering
Ecole Polytechnique de Montreal
Montreal,Quebec, H3T 1J4
Canada
Email: lionel.birglen@polymtl.ca

Carlos Ruella *
Robotics Laboratory
Department of Mechanical Engineering
Ecole Polytechnique de Montreal
Montreal,Quebec, H3T 1J4
Canada
Email: carlos.ruella@polymtl.ca

ABSTRACT

In legged mobile robotics the most common approach is to design fully actuated legs with several degrees of freedom (DOF) in order to successfully navigate through rough terrains. However, simpler leg architectures with as few as one-DOF have been developed in the past to achieve the very same goal. The ability of these simpler legs to traverse uneven terrains is arguably limited with respect to multi-DOF designs, but in some applications the reduction of the DOF and hence, of the number of actuators, as well as the simplicity of the associated control could be a great advantage and the decisive argument. In this paper, the authors propose a novel one-DOF robotic leg that has been specially designed to achieve the greatest robustness possible with respect to the difficult terrains it has to traverse. In order to do that, a method to analyze and optimize any one-DOF robotic leg with respect to its ability to overcome obstacles is proposed here. This method is based on a simple and efficient novel technique to generate synthetic terrains combined with a simulation algorithm estimating the traversability of the particular one-DOF leg design under scrutiny. To illustrate the generality of the proposed method, it is used to design both an optimal leg with the architecture presented here for the first time and also, one with the most common one-DOF leg architecture found in the literature.

INTRODUCTION

The advantages of legged robots over those using different locomotion systems lie in their ability of crossing difficult and rough terrains that other locomotion system, such as wheeled robots, might not be able to traverse [1, 2]. Unfortunately, the dexterity of legged robots comes with a price, namely a greater number of DOF per leg which makes them more expensive, less energy efficient and usually slower than most locomotion systems and in particular lower-DOF leg designs. In this work, a novel architecture of one-DOF robotic leg design is proposed. To evaluate its performance and come as close as possible to the ability of multi-DOF robotic legs to traverse difficult terrains, a method is also proposed here to simulate the behavior of any one-DOF leg architecture and optimize its geometric parameters to achieve optimal traversability. The final aim is to develop a legged robot capable of traversing different types of uneven terrains without the need of high-level control and with a reduced number of DOF.

Clearly, multi-DOF legs have generally better performance than one-DOF legs, mainly because the ability of the latter to adapt to the terrain is limited. Nevertheless, as mentioned before, in some applications the reduction of the number of actuators required is a more important design parameter, mainly because of the cost. For example in space exploration, where it is nearly impossible to replace a broken actuator, a legged robot equipped with multi-DOF legs, would be less reliable than one equipped with one-DOF legs, simply because it has less actua-

*Address all correspondence to this author.

tors that could fail. Additionally, less actuators per leg would reduce the weight of the robot and thus, it would be more energy efficient.

The state of the art in legged robots and most of the literature on this subject focuses on the control of the several DOF of each leg and the coordination between them [3]. Multi-DOF legged robots can indeed independently actuate each DOF of each leg to achieve a planned foot trajectory [4]. On the other hand, this present work aims at studying legs with only one-DOF. In such systems, the foot trajectory is defined by its geometrical parameters and cannot be altered once the mechanism is built. This makes the kinematic comparison between multi-DOF and one-DOF leg nearly impossible, mainly because the entire existing indexes in the literature assume architectures with several independently actuated DOF which is not the case for one-DOF legs. Hence, other metrics should be developed and used as it will be proposed here. Then, these metrics can be subsequently optimized.

In the literature, several works dealing with the estimation of the traversability of legged and wheeled robots can be found, [1, 5–8]. To simulate the interaction between a mobile robot and the terrain being traversed, certain commercially available dynamic simulation programs could be used, or a dedicated simulation algorithm could be developed. Regardless of the tool used to simulate this interaction, the synthesis of realistic virtual terrains is the key element in the simulation process.

When reviewing the methods of virtual terrain generation, it was noted by the authors that most articles and books on this subject belong to the field of graphic design for movie animation or video games. In this field, there is a common trend to use fractal methods to generate the terrains. One of the fractal methods widely used by graphic designers is the fractional Brownian motion (fBm). It is generally accepted as being an elegant and simple way to generate artificial terrains [9]. However, most papers in robotics often use simpler models of terrain. For example, the authors of [10] define a terrain as a set of constant size panels with randomly changing inclination angles within a certain range bounded by α_{min} and α_{max}. Similarly, in [7] panels are used to form the terrain and the elevation of each panel is again chosen randomly. These approaches do not generate terrains that "feel" natural and are often a coarse approximation of what can be found in the field.

OUTLINE OF THE PROPOSED METHOD

To analyze the traverse capability of a legged robot (referred here to as its traversability) over rough terrains, a new method to generate synthetic landscapes is detailed in the following section and compared to the most common one found in the literature. Then, the simulation algorithm presented, it analyzes step-by-step the walking process of the leg to obtain a performance index estimating the probability of this leg to traverse a specified terrain given a certain foot trajectory (both in force and position). This traversability index is used as the fitness objective function for a multivariate genetic algorithm optimization of the geometric parameters defining the leg.

In order to reduce the complexity and the computation time of the simulation, several assumptions are made. First, the simulation algorithm analyzes the walking of one leg only, instead of the four or six legs that usually compose a legged robot. It is assumed that assessing the traversability performance of one leg will provide a general idea of how well the robot, composed by several of these legs, will perform. This was also experimentally verified in preliminary experiments by the authors to be realistic. Second, since most of the robotic legs with few DOF have a planar architecture, the generated terrain is also a 2D profile. Finally, the terrain is considered solid.

TERRAIN MODELING

The method developed here to generate synthetic terrains uses the principle of Fourier series which reproduce a signal by means of the addition of simple sine functions. In our particular case, instead of having the usual time dependent signal, the terrain is regarded as position dependent signal. It should be noted that although in the present work only 2D profiles are considered, the method can be extrapolated to generate 3D synthetic terrains (cf. n-dimensional Fourier Transform).

The final goal is to produce synthetic terrains with similar geometric characteristics (e.g. smoothness) than these found in nature. In order to do so, the first step of the developed method is to take a digital photography of the desired terrain profile as a reference for future terrain generation. As shown in Fig. 1, a cardboard pattern of known size is also included in the picture allowing to find the ratio between the pixels in the picture and the real dimensions of the terrain in meters. The field of view of the camera is assumed to be small enough to neglect camera distortion.

FIGURE 1. Digital picture of an uneven terrain profile.

The next step is to extract the terrain profile from the picture. This can be done using any available picture editing software. The profile is subsequently transformed into a vector of positions

and heights in meters as illustrated in Fig. 2. In order to minimize the errors in the profile extraction, the known reference is placed as closely as possible to the image plane of the profile itself.

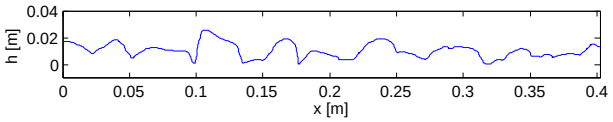

FIGURE 2. Terrain profile obtained from a vector representation.

Then, the power spectral density of the vector representing the terrain profile is computed. This power spectral density is the square of the magnitude of the discrete Fourier Transform of the signal. From the power spectral density, one is able to identify the principal harmonics (individual sine functions of known frequencies) of the terrain profile. Then, these harmonics with fundamental frequencies f_n, each with an amplitude A_n, are extracted and used in the next step, the terrain reconstruction.

To generate the synthetic terrain, a simple addition of sine functions with the frequencies and amplitudes extracted from the power spectral density is performed, i.e.:

$$terrain(x) = \sum_{n=1}^{N} A_n \sin\left(f_n x + \Theta_{rand}\right), \tag{1}$$

where $terrain(x)$ is the height at each point x of the newly generated terrain.

In order to generate several different terrains, a random phase (Θ_{rand}) is added to each sine functions. This phase has a random numerical value between 0 and π so that each generated terrain has a different shape but the same power spectrum in amplitude. The number of harmonics used in the terrain reconstruction is controlled by the parameter N in the previous equation. It was noted that, using only the quarter of the harmonics corresponding to the lower frequencies is generally enough to create synthetic terrains similar to the original one from the digital picture. The higher frequency harmonics correspond to noise produced by different sources in the terrain profile capture and editing processes.

By discarding the higher frequency harmonics some small perturbations of the natural terrains (mostly dust and loose soil particles) will not appear in the simulated terrain. However considering the scale of those perturbations compared with the size of the legs, it was assumed that they do not significantly impact slippage and collisions. Additionally, due to the continuous nature of the Fourier series, certain terrain shapes (mostly artificial) cannot be accurately modeled, for instance those with sharp edges. Indeed, in the latter case, the Gibbs phenomenon presents a realistic modeling even when a large number of harmonics is considered. The method presented here is therefore not suited to be used when simulation steps for example.

Using the above method, a library of different terrains with the same characteristics as the original one can be produced. Fig. 3 presents an example of a synthetic terrain produced from the data obtained from Fig. 2. The resemblance between the geometries of the original and synthetic landscape profiles can be readily observed.

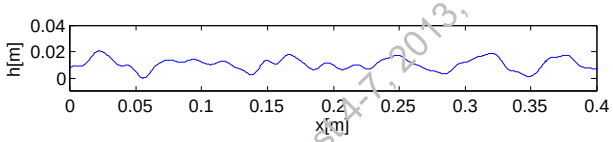

FIGURE 3. Generated synthetic terrain.

The method presented here has a more time-consuming first step (sampling the initial terrain picture) than the methods used in the literature, e.g. [10] or [7]. However, it produces an infinite number of terrains with similar characteristics to the one initially used. This is a clear advantage because if a simulation environment is used, testing a design over a large number of terrains is capital to ensure robustness. As a consequence, a design that performs well in the simulation using this multitude of terrains will most likely also have the same performance in the field [11].

As mentioned earlier, Brownian motion is a mathematical model often used to represent real terrains, e.g. [8]. In the latter, a real terrain profile was captured by means of a laser range finder, from which a power spectral density was also computed. From these data two parameters, H and σ, were extracted to build a synthetic terrain. This method uses a more expensive procedure to capture the real terrain profile than our approach, and uses only those two parameters to perform the reconstruction of a virtual terrain. Using the method developed in this paper the terrain reconstruction takes more information from the power spectral density which results in a synthetic terrain that more closely resembles the original terrain profile.

In order to compare the terrains produced by our method and the ones produced by the Brownian motion model such as in [8], their power spectral density can be analyzed and compared. In general, the Brownian motion is represented as a time dependent random function $V(t)$ with the following power spectral density:

$$S(f) = \frac{\sigma^2}{f^{2(H+1)}}, \tag{2}$$

where σ is the standard deviation of a Gaussian distribution, f is the frequency and H is a parameter known as the Hölder exponent. The power spectral density of the terrains produced by the

method presented in this paper is directly the one of the terrain profile, i.e.:

$$S(f_n) = A_n. \tag{3}$$

To test if the proposed method produces closer looking terrains than those produced by the Brownian motion, instead of reproducing the initial terrain from a photo of a profile, the fundamental amplitudes used for the reconstruction were forced to the equivalent values of the Brownian model using the following equation:

$$A_n = \frac{\sigma^2}{f_n^{2(H+1)}}, \tag{4}$$

where H and σ were taken from two examples of real terrains given in [8]. In the latter work H and σ were identified for a terrain composed by gravel and one composed by chopped bricks. In Table 1, the parameters obtained by [8] are presented as well as the first four fundamental amplitudes for the two terrains computed using Eq. 4.

TABLE 1. fBm parameters and their respective A_n

	H	σ	A_1	A_2	A_3	A_4
Gravel	0.33	0.0035	24.2	27.8	29.6	32.4
Chopped bricks	0.36	0.0080	43.4	49.4	56.2	66.3

With the fundamental amplitudes computed for both the gravel and the chopped brick terrains, the reconstruction of these virtual terrains using the method proposed in this paper and the standard Brownian motion were done. The resultant terrains are presented in Fig. 4. From this figure one can readily observe that both methods produced similarly looking profiles. However, the main advantages of the proposed method are that it is simpler to acquire the natural terrain profile, it requires a lower cost apparatus (only a digital camera is needed) and it is also less time consuming. Yet, it produces similar results.

TRAVERSABILITY SIMULATION

An algorithm estimating the traversability of one-DOF robotic legs over a specified terrain is presented in this section. This algorithm has a modular structure to be able to simulate various mechanical leg architectures crossing over several different types of terrains. It receives as inputs: the geometry of the

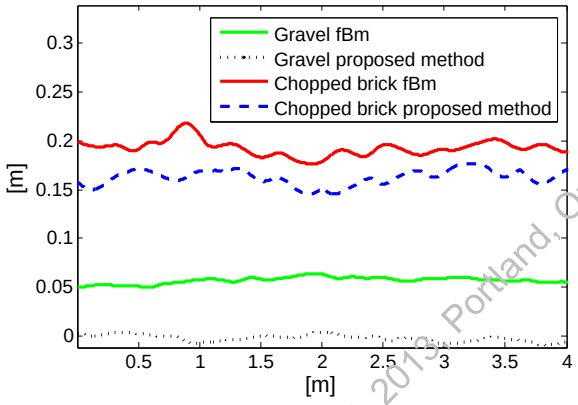

FIGURE 4. Proposed method and Brownian motion comparison.

terrain, the initial position where the leg starts its walk, the trajectory of the foot, and the force that the leg is able to apply to the terrain in each point of its trajectory. Note that the design of the leg itself is not used, only the generated foot position trajectory and the force applied along the later. The traversability simulation was specifically developed for leg architectures with one-DOF. This makes our custom simulator faster and more efficient than commercially available simulators that are designed for general problems.

For each leg architecture, the trajectory of the foot has to be computed by means of the direct kinematics beforehand. Next, the force along the trajectory that the leg is able to generate is computed using the principle of virtual work [12].

Then, the simulation algorithm analyzes each step sequentially from the initial position to the end of the terrain. It starts by determining whether the initial position of the foot is a stable point of contact or not. A stable point is defined as any position on the terrain where the foot can be placed without slippage. To determine if the foot slips over the terrain, the friction force between the foot and the terrain is assumed to follow the Coulomb friction law. When a point is not stable the direction of slippage is determined and the stability of the next point where the foot has slipped is tested. This procedure is repeated until a stable point is found.

Before going into the details of the algorithm, the main characteristics of the trajectory of a foot must be defined. First, the step length is defined as the distance between the maximal and minimal points in the abscissa of the trajectory. Its clearance is considered to be the distance between the maximal and minimal points along the ordinate axis. The trajectory is divided in two phases: the flying phase and the support phase as illustrated in Fig.5.

During the flying phase of the trajectory the algorithm checks if a collision occurs between the foot and the terrain. If there is no collision the step is considered valid. Any contact between the terrain and the foot during the support phase of the

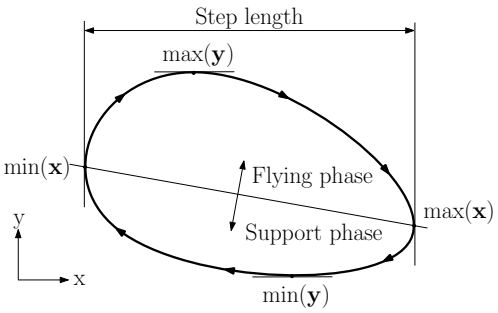

FIGURE 5. Example of a foot trajectory.

trajectory is defined as a landing. If this occurs, the stability of the point where the foot landed is analyzed again. It should be noted that a step where a collision takes place during the flying phase is considered invalid, even if the leg was able to move the robot forward a certain distance. Because the terrain and the leg structure are considered solid, when a collision occurs the body of the robot move backward as it reacts to the collision. The body is displaced backward the same distance that the foot would have move forward from the collision point to the end of the flying phase. Hence, the foot position after the collision is recalculated considering this displacement. This iterative process is repeated until the leg completely traverses the terrain.

A simulator implementing this algorithm has been developed and is capable of plotting the walking process of the leg as illustrated in Fig. 6. Some of the situations previously discussed can be clearly seen in the latter figure. For example, the step number 1 collides with the terrain and therefore, step number 2 starts where the foot backed down as a consequence of the collision. Also, during step number 2 the position where the foot lands is unstable. Slippage then occurs until the foot reaches a stable point downward the slope of the terrain.

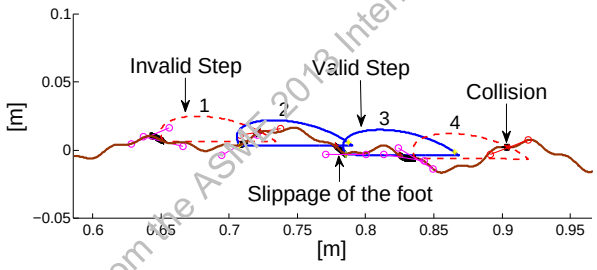

FIGURE 6. Examples of valid/invalid steps.

The traversability index (T_{ind}) proposed in this paper is a value between zero and one evaluating the capability of a leg to traverse a given terrain. A T_{ind} of zero means that the leg is not able to cross the terrain. In the best case scenario, when neither collision nor slippage occurred, the leg obtains a T_{ind} equals to one. To compute the traversability index, the number of valid and invalid steps is used, namely:

$$T_{ind} = \left(\frac{V_s}{I_s + V_s}\right)\left(\frac{L_t}{(I_s + V_s)\,L_s}\right), \tag{5}$$

where V_s and I_s are respectively the number of valid and invalid steps, L_t is the length of the terrain and L_s is the length of the step. The first part of Eq. (5) is the ratio between the valid and invalid steps. This ratio allows to quantify the percentage of invalid steps that took place during the simulation. Ideally, when all steps are valid this ratio is equal to one. The second factor of Eq. (5) is an efficiency ratio, a key element in the design of legged robots.

As mentioned before, most of the performance indices proposed in the literature are not adapted to evaluate one-DOF legs. Nevertheless, the efficiency ratio as previously defined in Eq. (5) was inspired from an index referred to as the specific resistance, an important dimensionless number used to evaluate the energy efficiency of a mobile robot. It is usually computed as follows:

$$\varepsilon = \frac{E}{Mgd}, \tag{6}$$

where E is the total energy consumption required for traveling a distance d, M is the total mass of the robot and g is the acceleration due to gravity. Assuming that, on average, every step requires the same amount of energy, the second factor of the traversability index is actually related to ε as defined in the literature.

OPTIMIZATION OF THE GEOMETRIC PARAMETERS

In one-DOF robotic legs, the trajectory described by the foot and the force is able to apply to the terrain depend mainly on the control scheme of the actuator and the geometric parameters defining its architecture. The actuator can be appropriately controlled while the robot is walking. On the other hand, the geometric parameters of the leg once built, are constant. With the aim of developing robotic legs that do not require a complex control strategy for their actuator, a careful optimization of the geometric parameters of the legs must be done.

In the literature one can find several performance indices used to evaluate legged robots, the authors of [13] presented a summary of the most frequently used indices, such as the stability margin, the Froude number, the duty factor and the specific resistance. Nevertheless, most of those indices depend on the type of gait and stance that the robot uses to walk. As it is aimed here to optimize only one leg and not a full walking robot, it was impossible to use the documented indices since they rely on the gait of the robot.

As detailed in the previous section, the developed simulator outputs a traversability index, i.e. a number between 0 and 1. This index could be used to optimize the geometric parameters of the legs. However, when this optimization metric was first tested it yielded geometric parameters with several singularity points along the foot trajectory which would cause mechanical stress in the joints and in the actuator as well. To solve this issue, four additional performance indices are subsequently defined as functions only of the leg, without taking into consideration the terrains. This was also done in order to obtain an optimal design considering more precisely certain characteristics of the foot trajectory such as smoothness, clearance, strike and force.

The smoothness of the trajectory is defined here as the maximal variation of the tangent angle of the latter. This value is normalized over 2π in order to obtain values between 0 and 1. The clearance and strike are simply defined as the distances between the minimal and maximal points of the trajectory respectively in the abscissa and ordinate axis. Both of these values are normalized with respect to $2L$, where L is the maximal length of the leg when extended. These normalizations are also made to obtain values between 0 and 1. Finally, the force index is the average of the magnitude of the force that the leg is able to apply to the terrain. This index is again normalized over the maximal force along the trajectory to be consistent with the other geometrical indices.

Using the traversability index obtained from the developed simulator together with the four indices depending only on the geometric parameters, a combined global performance index may be defined, e.g.:

$$I_{global} = \frac{1}{T_{ind}} + I_{geo}. \tag{7}$$

where I_{geo} is the combination of the performance indices, previously defined, depending only on the geometric parameters of the leg. I_{global} is to be minimized (the optimization algorithm minimize its objective function). The type of optimization suggested in this paper is based on a genetic algorithm, a technique well suited to this type of problem because it is capable of finding a solution, even when the analytical expressions are impractical or cannot yield an exact solution [14].

The optimization problem is defined as follows:

$$\min_{\mathbf{x}\in\Omega} f(\mathbf{x}) \tag{8}$$

where $\mathbf{x}$ is the vector containing all the geometric parameters, Ω represents the feasible geometric parameter space and f is the function which receives as input the geometric parameters of a leg and outputs its global performance index I_{global}.

In order to obtain a leg able to cross over different types of terrains, the optimization process is repeated over five different types of terrains generated using the terrain generation method proposed in this paper. Additionally, to obtain an accurate traversability index, the walking process of the leg is simulated over 10 terrains of each type, yielding a total of 50 terrains. Then, the average traversability is computed. When designing a walking robot the types of terrain which the robot is supposed to cross are one on the main design requirement.

As mentioned before in this work, the legs were design using five types of terrains as requirement. Nevertheless, the method could be extended to use more terrains. However, if the resultant leg is tested over terrains far different from the terrains used as requirement during the design process, is clear that the leg will not perform as well. The same would arrive with any other mechanisms use in conditions that were not taken in consideration during its design.

In order to determine the minimum number of the same terrain over which the simulation has to be performed to guarantee a small standard deviation for the traversability, 10 sets of different geometric parameters were simulated over 2, 5, 10, 20 and 40 terrains. It was noted that for 10 or more terrains, the standard deviation was always smaller than 5%. For this reason each leg architecture is consequently tested over 10 terrains of the same type.

SIMULATION AND OPTIMIZATION EXAMPLES

The terrain generation method and the simulation algorithm were used to analyze the traversability, optimize the geometric parameters and compare the performance of a novel architecture developed by the authors called the RuBi leg to the commonly found Chebyshev leg. With the aim of comparing the performances of both legs, two lengths in each leg were fixed to constant values. These lengths being fixed did not participate as variables in the optimization process. The two lengths were chosen in order for both legs to share the same maximal length from foot to base when fully extended.

RUBI LEG

The RuBi leg was inspired by the simplicity of the Chebyshev leg and the simplified two-link model of a mammal leg [15]. It is shown in Fig. 7, the resemblance with the Chebyshev leg (c.f. Fig. 8) is clear. The point P_1 describes the same trajectory as the foot of an inverted Chebyshev leg. However, this leg has a second link, and the same transmission mechanism that drives the first link also drives the second one. Therefore, the angles θ_1 and θ_2 are coupled.

The position of the foot of the RuBi leg can be calculated

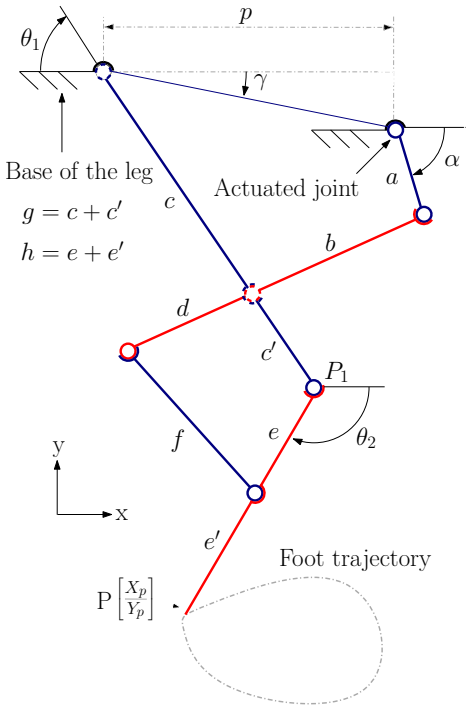

FIGURE 7. RuBi leg.

using simple trigonometry, namely:

$$X_p = g\cos\theta_1 + h\cos\theta_2, \tag{9}$$

$$Y_p = g\sin\theta_1 + h\sin\theta_2, \tag{10}$$

where θ_1 and θ_2 are the angles of the main links of the leg with respect to the x-axis of the reference frame. To compute the angles θ_1 and θ_2, the loop-closure equations yield:

$$\theta_1 = \arccos\left(\frac{R}{E}\right) + \arctan\left(\frac{2K_2 + 2a\sin\alpha}{2K_1 + 2a\cos\alpha}\right), \tag{11}$$

$$\theta_2 = \arctan\left(\frac{P}{Q}\right) - \arccos\left(\frac{M}{2e\sqrt{Q^2+P^2}}\right), \tag{12}$$

where R, E, Q, P, M, K_1 and K_2 are computed as follows:

$$\begin{aligned} R = &-K_1^2 - 2K_1 a\cos\alpha - K_2^2 - 2K_2 a\sin\alpha \\ &- a^2 - c^2 + b^2, \end{aligned} \tag{13}$$

$$E = 2c\sqrt{(K_2 + a\sin\alpha)^2 + (K_1 + a\cos\alpha)^2}, \tag{14}$$

$$Q = -c\cos\theta 1 - d\cos(\theta 1 + \Phi) + A\cos\theta 1, \tag{15}$$

$$P = -c\sin\theta 1 - d\sin(\theta 1 + \Phi) + A\sin\theta 1, \tag{16}$$

$$\begin{aligned} M = &2dA\sin(\theta 1 + \Phi)\sin\theta 1 + 2Ad\cos(\theta 1 + \Phi)\cos\theta 1 \\ &+ 2cA + f^2 - 2cd\sin\theta 1\sin(\theta 1 + \Phi) \\ &- d^2 - A^2 - e^2 - c^2 - 2cd\cos\theta 1\cos(\theta 1 + \Phi), \end{aligned} \tag{17}$$

$$K_1 = p\cos\gamma, \tag{18}$$

$$K_2 = p\sin\gamma. \tag{19}$$

The angle Φ is computed as follows:

$$\Phi = \arccos\left(\frac{1 + b^2 + c^2}{2bc}\right). \tag{20}$$

It is important to mention that due to the non-unique solution of the arccos and the arctan functions, Eqs. (11), (12) as well as the angle Φ have several possible values. Nevertheless, there is only one configuration producing a feasible mechanism.

The lengths p, a, b, c, d, e, f, g, h and the angle γ are the geometric parameters of this leg. The angle α is the actuator angle, as illustrated in Fig. 7. Afterwards, knowing the Cartesian position of the foot as a function of the actuator angle, the inverse ratio between the displacement of the foot and the angular displacement of the actuator (also known as the mechanical advantage) can be computed, i.e.:

$$R_i = \frac{\Delta\alpha_i}{\Delta s_i}, \tag{21}$$

where Δs_i is the displacement of the foot due to an angular displacement of the actuator $\Delta\alpha_i$ for $\alpha_i = [0, 2\pi]$. Using the principle of virtual work, to compute the magnitude F_i of the force generated at the foot (in each point of its trajectory) one must

multiply the actuator torque T_a, assumed constant, by the previous ratio, i.e.:

$$F_i = T_a R_i. \tag{22}$$

With the equations to compute the foot trajectory and the force which the foot is able to apply to the terrain, the geometric parameters of the leg can be optimized using the previously described method in order to obtain the best possible traversability performance for this particular architecture. When optimizing the geometric parameters of this leg, the two lengths chosen to be constant are g, set to $100[mm]$, and h, set to $86[mm]$. For this architecture the optimized parameters found were: $a = 18.3[mm]$, $b = 59.7[mm]$, $c = 69.9[mm]$, $d = 30.6[mm]$, $e = 34.8[mm]$, $f = 44.5[mm]$, $p = 95.8[mm]$ and $\gamma = -2.3°$.

CHEBYSHEV LEG

The Chebyshev leg is one of the most common and oldest architecture for legged robots with one-DOF and is illustrated in Fig. 8, described in [16, 17]. Many mobile robots with one-DOF legs use the Chebyshev architecture as an element, cf. [18–21].

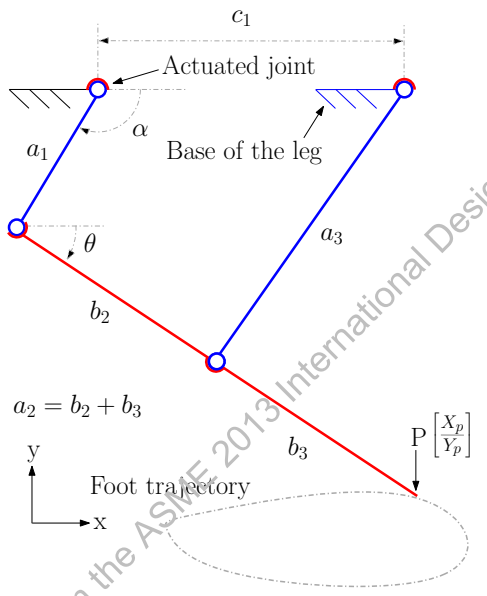

FIGURE 8. Chebyshev leg.

The computation of the foot position for this leg can be found in the literature, e.g. [22]. The force that the foot is able to apply to the terrain is computed again by means of the virtual work principle using Eq. (22). The optimization of the geometric parameters of this leg was done using exactly the same methodology as with the RuBi leg. The only difference is obviously the number of parameters to be optimized. The two lengths chosen to be constant for the optimization process, are here a_3, set to $100[mm]$, and b_3, set to $86[mm]$. For this leg, the obtained optimal lengths are: $c_1 = 119.5[mm]$, $a_1 = 16[mm]$ and $b_2 = 60.2[mm]$.

In the literature, e.g. [19, 21], the lengths b_2 and a_3 of the Chebyshev leg are often chosen equal which is not the case here. As mentioned earlier, to compare the Chebyshev and RuBi leg, two dimensions of each leg were fixed. For the Chebyshev leg it was a_3 and it was expected that the optimal value for b_2 would be close to the value of a_3 as previously seen in the literature. However, the optimization process discussed in the paper found that b_2 should be actually 40% smaller than a_3 to yield the best performance.

CHEBYSHEV LEG AND RUBI LEG COMPARISON

It is important to insist that due to the one-DOF nature of both legs analyzed in this paper, comparing them to other multi-DOF legs would be unfair for a number of reasons as previously explained. That is the main reason why another one-DOF leg was chosen to be compared to the Rubi leg. The Chebyshev leg was used since it is the base for most one-DOF robotic leg architectures.

Both legs considered in this paper were tested over seven types of terrains: a flat terrain, a terrain with gentle slopes in the form of a sinusoidal function with low frequency, and five more "natural" terrains with different roughness levels. These last five types of terrains were generated with the method proposed in this paper. All the results are shown in Table 2. The sinusoidal and the flat terrains are respectively terrain number one and two while the uneven terrains are ordered as a function of their roughness (i.e. terrain number three is the smoother and number seven is the roughest).

TABLE 2. Traversability index of each leg in the seven terrains in [%]

Terrain #	1	2	3	4	5	6	7
Chebyshev leg	88	88	88	84	60	40	3
RuBi leg	75	75	75	82	62	48	16

As expected, in certain terrains one architecture is better than the other. Nevertheless, the difference in traversability is not very significant because the two legs were optimized using the same optimization indices and, additionally, they share the same length when extended. For the terrains four, five and six the traversability of both legs decreases as the terrains get more uneven.

Even though the Chebyshev leg has an overall better performance for easy terrains, the RuBi leg showed a better traversability over the roughest terrains (numbers five, six and seven). As shown in the table, the less uneven (number three), flat, and the sinusoidal terrains obtained similar traversability indices. Please note that the index is not 100% for the flat terrain as could be expected. This results from the efficiency ratio in the traversability index equation: the legs were optimized to cross rough terrains and if they are able to traverse a flat terrain without any collision, they are not very efficient for this task since it takes them many steps compared to the length of the traversed distance.

CONCLUSION

In this paper, the authors proposed a novel one-DOF robotic leg architecture based on the Chebyshev leg, a new terrain generation method, as well as a traversability simulation algorithm. The synthetic terrain produced using the developed method held characteristic similar to real terrains, where the robot will walk. The novel leg architecture presented by the authors was compared with the Chebyshev leg, one of the most common one-DOF robotic leg architecture. We concluded that for difficult terrains the RuBi leg performs better than the Chebyshev leg. In addition, the proposed traversability simulations together with the optimization algorithm could help to enhance the performances of any one-DOF leg architectures.

ACKNOWLEDGMENT

The financial support of the Natural Science and Engineering Research of Canada (NSERC) and the Canadian Foundation for Innovation (CFI) is gratefully acknowledged.

REFERENCES

[1] Loc, V.-G., Koo, I. M., Trong, T., Kim, H. M., Moon, H., Park, S., and Choi, H. R., 2010. "A study on traversability of quadruped robot in rough terrain". In International Conference on Control Automation and Systems (ICCAS), pp. 1707–1711.

[2] Remy, C. D., 2010. "Walking and crawling with alof: a robot for autonomous locomotion on four legs". In Proceedings of CLAWARD: 13th International Conferece on Climbing and Walking Robots and the Support Technologies for Mobile Machines, Vol. 38, pp. 264–268.

[3] Waldron, K. J., Estremera, J., Csonka, P., and Singh, S. P. N., 2009. "Analyzing bounding and galloping using simple models". *Journal of Mechanisms and Robotics,* ***1***, pp. 1–11.

[4] Nichol, J. G., Singh, S. P., Waldron, K. J., Palmer, L. R., and Orin, D. E., 2004. "System design of a quadrupedal galloping machine". *The International Journal of Robotics Research,* ***23***, pp. 1013–1027.

[5] Gu, J., Cao, Q., and Huang, Y., 2008. "Rapid traversability assessment in 2.5d grid-based map on rough terrain". *International Journal of Advanced Robotic Systems,* ***5***(4), pp. 389–394.

[6] Li, W., Huang, Y., Cui, Y., Dong, S., and Wang, J., 2010. "Trafficability analysis of lunar mare terrain by means of the discrete element method for wheeled rover locomotion". *Journal of Terramechanics,* ***47***(3), pp. 161–172.

[7] Palmer, L., and Orin, D., 2007. "Quadrupedal running at high speed over uneven terrain". In IEEE/RSJ International Conference on Intelligent Robots and Systems. IROS, pp. 303–308.

[8] Yokokohji, Y., Chaen, S., and Yoshikawa, T., 2004. "Evaluation of traversability of wheeled mobile robots on uneven terrains by fractal terrain model". In Proceedings of the IEEE International Conference on Robotics and Automation. ICRA, Vol. 3, pp. 2183–2188.

[9] Deussen, O., and Lintermann, B., 2005. *Digital Design of Nature Computer Generated Plants and Organics*. X.media.publishing, ch. Modeling Terrain, pp. 113–123.

[10] Amagata, Y., Nakaura, S., and Sampei, M., 2008. "The running of humanoid robot on uneven terrain utilizing output zeroing". In SICE Annual Conference, Technische Universiteit Eindhoven, pp. 2841–2846.

[11] Lipson, H., Bongard, J., Zykov, V., and Malone, E., 2006. "Evolutionary robotics for legged machines: From simulation to physical reality". In Proceedings of the 9th Int. Conference on Intelligent Autonomous Systems., pp. 11–18.

[12] Spong, M. W., Hutchinson, S., and Vidyasagar, M., 2005. *Robot Modeling and Control*. John Wiley & Sons, Inc.

[13] Kajita, S., and Espiau, B., 2008. *Handbook of Robotics*. Springer, Berlin-Heidelberg, ch. Legged Robots, pp. 361–389.

[14] Whitley, D., 1994. *A Genetic Algorithm Tutorial*, samizdat press ed. Computer Science Department, Colorado State University, Fort Collins, Co 80523.

[15] Francesco, C., 1994. Desing and simulation of an all terrain mobile robot. Tech. rep., The university of Leeds.

[16] Artobolevsky, I., 1989. *Mechanisms in modern engineering design*, Vol. I-III. MIR Publisher Moscow.

[17] Raibert, M. H., 1986. "Legged robots". *Communications of the ACM,* ***29***(6), pp. 499–514.

[18] Tavolieri, C., Ottaviano, E., Ceccarelli, M., and Rienzo, A. D., 2006. "Analysis and design of a 1-dof leg for walking machines". In The 15th International Workshop on Robotics in Alpe-Adria-Danube Region (RAAD).

[19] Shieh, W., Tasai, L., and Azarm, U., 1997. "Design and optimization of a one-degree-of-freedom six-bar leg mechanism for a walking machine". *Journal of Robotics systems,*

14(12), pp. 871–880.

[20] Kendry, J. M., 2008. "Design and analysis of a class of planar biped robots mechanically coordinated by a single degree of freedom". *ASME Journal of Mechanical Design,* ***130***, p. 102302.

[21] Tavolieri, C., Ottaviano, E., Ceccarelli, M., and Rienzo, A. D., 2007. "A design of a new leg-wheel walking robot". In Mediterranean Conference on Control & Automation.

[22] Ottaviano, E., Lanni, C., and Ceccarelli, M., 2004. "Numerical and experimental analysis of a pantograph-leg with a fully-rotative actuating mechanism". In Proceedings of the 11th World Congress in Mechanism and Machine Science, pp. 1537–1541.